Supporting Information

A multifunctional Co-based metal-organic framework: heterogeneous catalysis, chemiluminescence sensing and moisture dependent solvatochromism

Authors: Ming-Hua Xie,[†] Ya Wang,[†] Ruo-Fei Li, [†] Peng-Yu Dong, [†] Gui-Hua Hou,[†] Rong Shao, [†] Xin-Guo Xi,[⊥] Rong-Feng Guan[†*] and Xiu-Li Yang[†*]

Affiliations:

[†]Key Laboratory for Advanced Technology in Environmental Protection of Jiangsu Province, Yancheng Institute of Technology, Yancheng, 224051, P. R. China

[⊥]School of Chemistry & Chemical Engineering, Yancheng Institute of Technology, Yancheng, P. R. China

*Correspondence to: xlychem@126.com

General information:

All reagents used in this work were commercial available and were used as received without further purification unless otherwise mentioned.

Determinations of the unit cell and data collection for crystal of CBBA-Co were performed at 293 K on a Bruker SMART-1000 CCD diffractometer using FRAMBO/SAINT software. The data were collected using graphite-monochromatized Cu radiation (λ=1.54178 Å). The structure of CBBA-Co was solved by direct methods, and refined by full-matrix least-square methods with the SHELX-2017/1 program package. The non-hydrogen atoms were refined anisotropically, and the H atoms bonded to carbon were generated geometrically. Thermogravimetric analyses (TGA) were carried out under a N_2 atmosphere on a PerkinElmer STA 8000 instrument at a heating rate of 10 $°C \cdot min^{-1}$. PXRD data were recorded on a X'Pert3 Powder for Cu Kα radiation (λ = 1.5406 Å). GC analysis were performed on a FULI GC 9790II gas chromatograph equipped with an SE-54 capillary column and a FID detector. H_2O_2 sensing study was performed on a MPI-II chemiluminescence analyzer. CO_2 adsorption/desorption isotherms were recorded on a Quantachrome Autosorb-iQ-TCD gas adsorption analyzer. Mass studies of CBBA-Co were performed on an SRS QCM-200 quartz crystal microbalance.

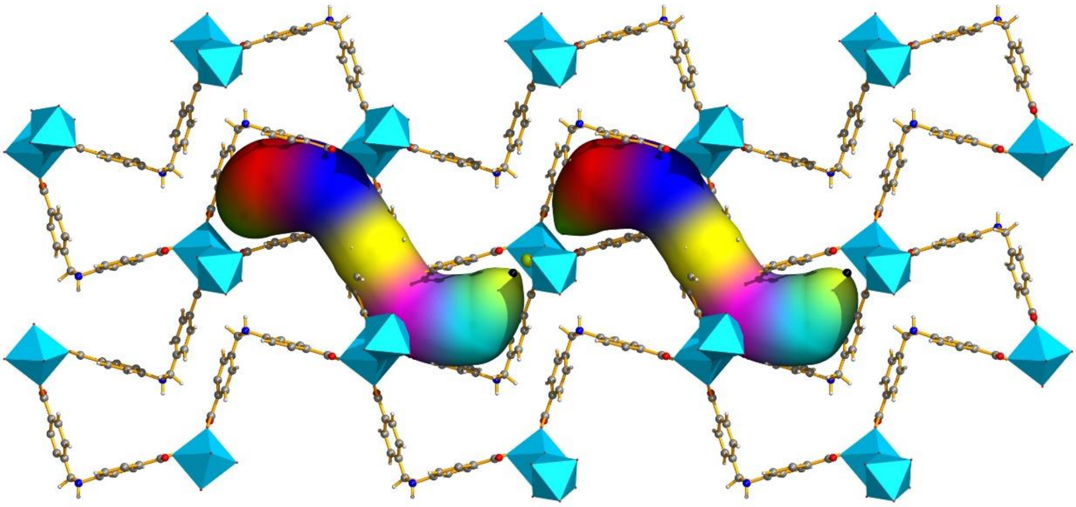

Figure S1. The zigzag pore structures of CBBA-Co as viewed down the *a* axis.

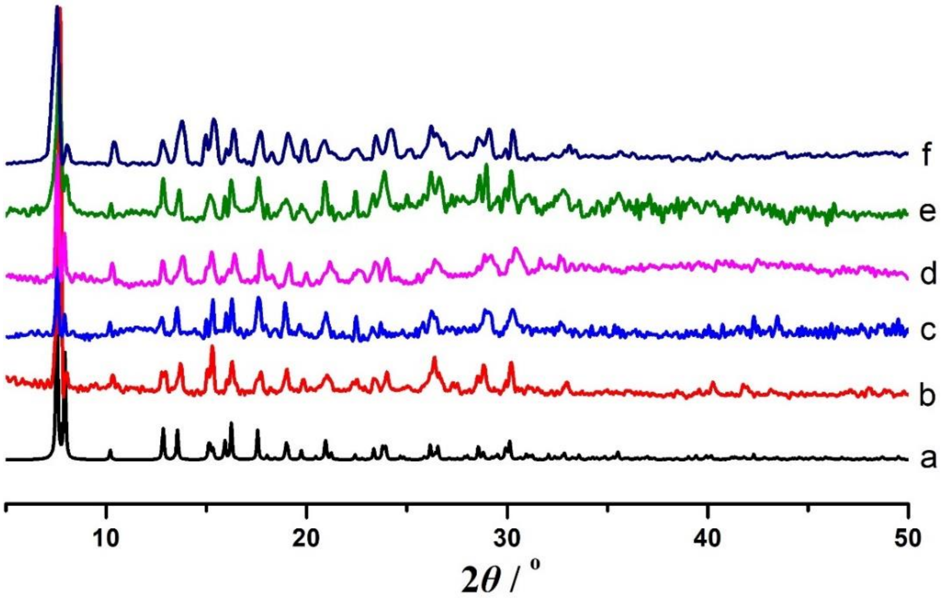

Figure S2. Powder X-ray diffraction patterns of CBBA-Co. a) simulated; b) as-prepared; c) fully-dehydrated; d) after ROR catalysis; e) after sulfide oxidation catalysis; f) after the lunimol chemiluminescence application.

Table S1. Crystal data and structure refinements for CBBA-Co.

Compound	**CBBA-Co**
Formula	$C_{36}H_{44}Co_3N_4O_{16}$
M	965.54
Temperature (K)	293(2)
Wavelength (Å)	1.54178
Crystal size (mm)	0.25 × 0.12 × 0.10
Crystal system	Monoclinic
Space group	$P2_1/c$
a (Å)	6.3974(5)
b (Å)	13.7521(13)
c (Å)	22.3408(19)
α (°)	90.00
β (°)	96.473(2)
γ (°)	90.00
Volume (Å^3)	1953.0(3)
Z	2
F(000)	994
θ for data collection (°)	3.78 to 66.04
Limiting indices	-7<=h<=7, -16<=k<=16, -4<=l<=26
Data / restraints / parameters	3380 / 86 / 286
Goodness-of-fit on F^2	1.050
R_1 (wR_2) [$I > 2\sigma(I)$]	0.0996 (0.2436)
R_1 (wR_2) (all data)	0.1420 (0.2773)

$R_1 = \sum(|F_o| - |F_c|) / \sum|F_o|$, $wR_2 = [\sum[w(F_{o2} - F_{c2})_2] / \sum w(F_{o2})_2]_{0.5}$

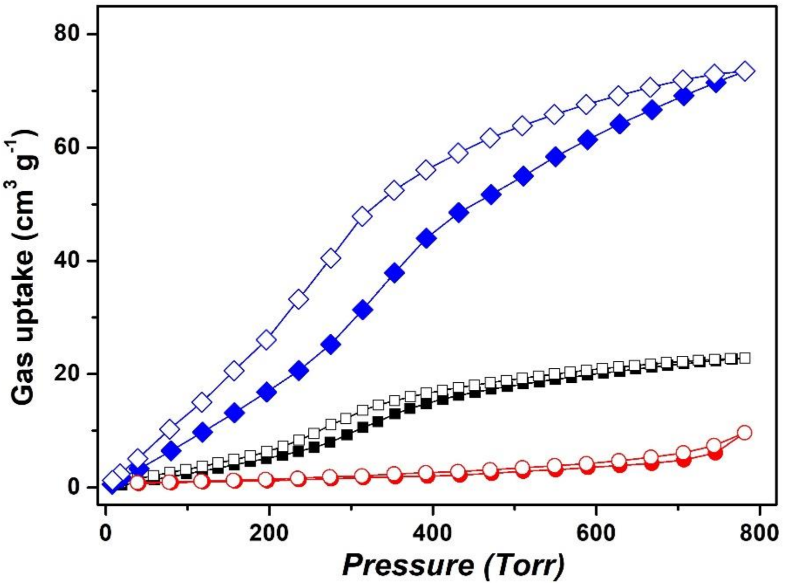

Figure S3. CO_2 adsorption/desorption isotherms for evacuated CBBA-Co at 195 K (blue), at 273 K (black) and N_2 adsorption/desorption isotherms at 77 K (red).

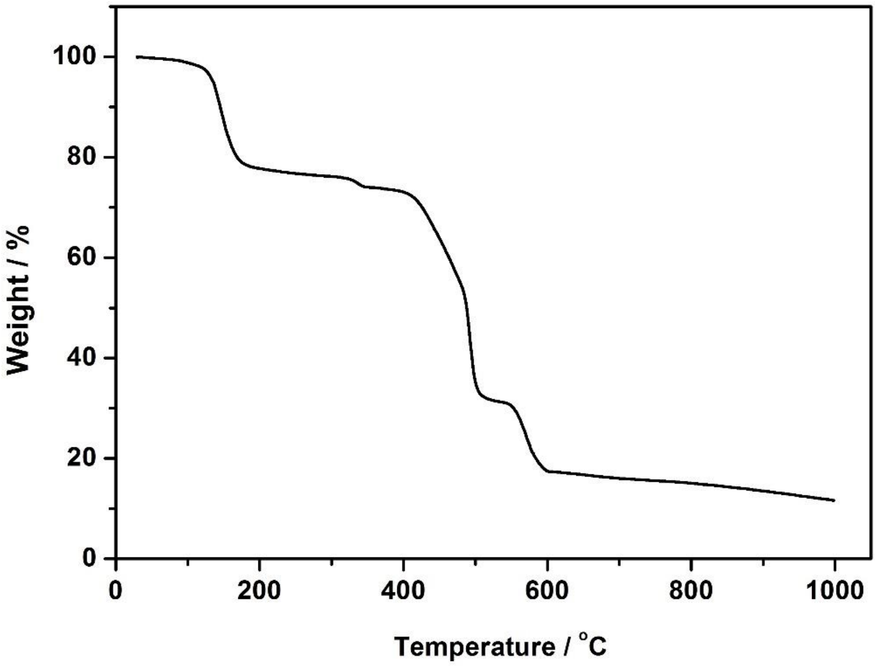

Figure S4. Thermal gravity analysis of CBBA-Co.

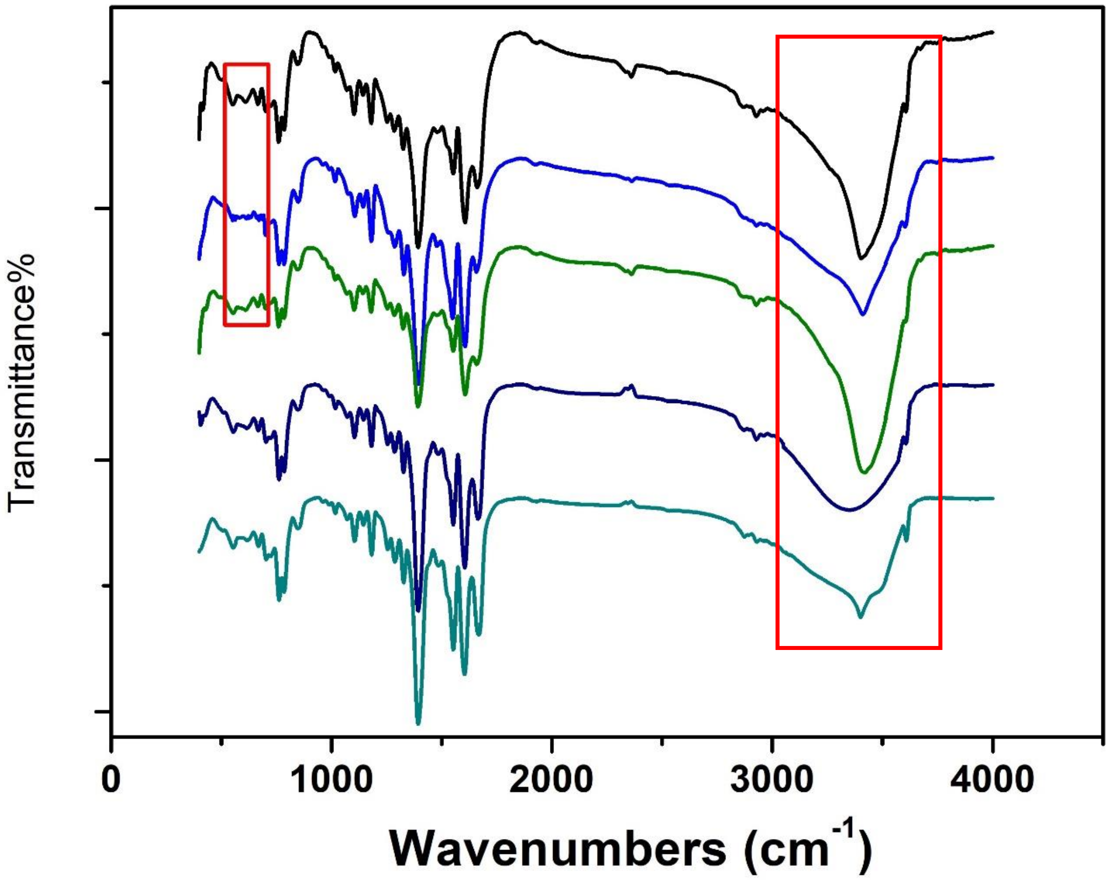

Figure S5. FT-IR spectrum of CBBA-Co after different treatment. From top to bottom: as prepared CBBA-Co, fully dehydrated CBBA-Co, rehydrated CBBA-Co, CBBA-Co during ROR catalysis and CBBA-Co during sulfide oxidation catalysis.

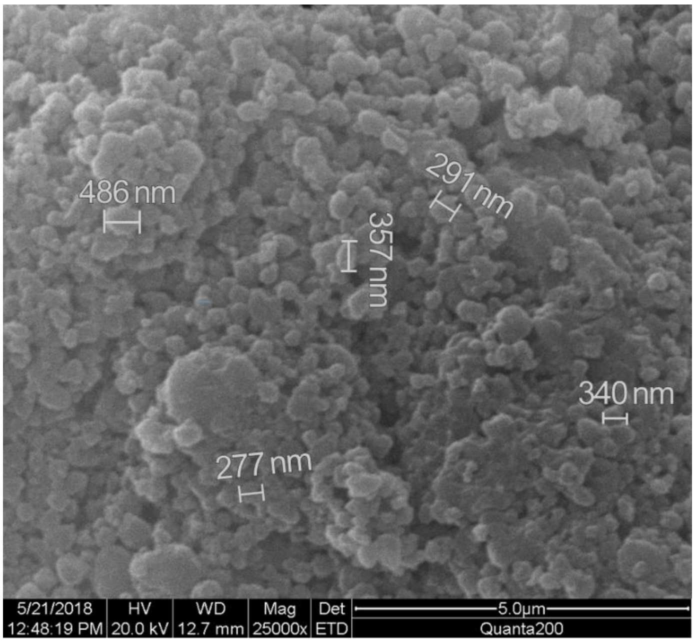

Figure S6. SEM image of the quartz crystal coated with CBBA-Co nano particles.

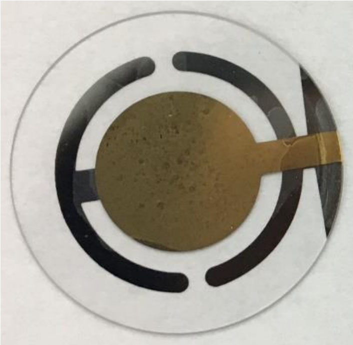

Figure S7. Image of the quartz crystal coated with CBBA-Co thin film.

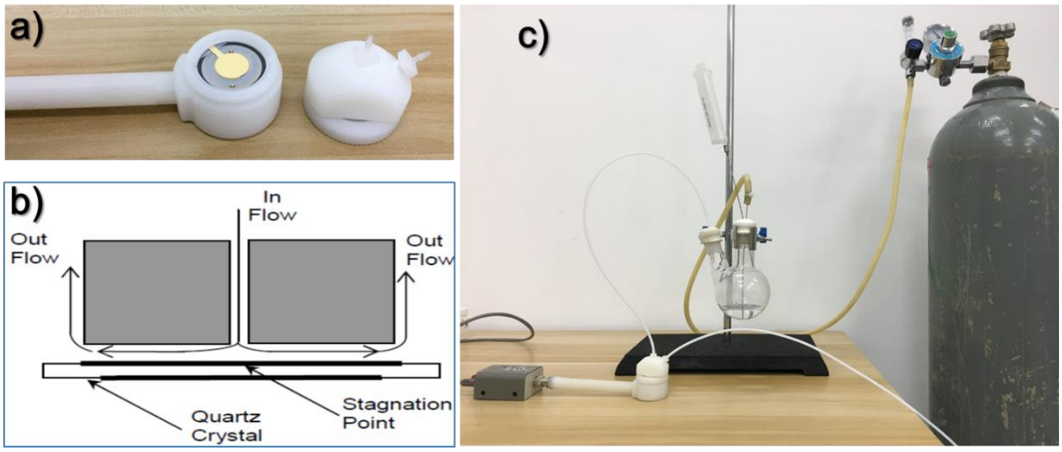

Figure S8. CBBA-Co adsorption test by QCM. a) image of coated 1 inch quartz crystal equipped in a flow cell adapter; b) Schematic representation of the flow pattern in the flow cell; c) Experimental set up of QCM tests

Table S2. Molecular size of substance used in the QCM test

Entry	Substance	Structure and size
1	**H_2O**	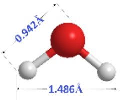
2	**DMF**	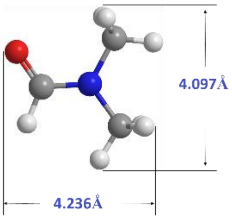
3	**TBHP**	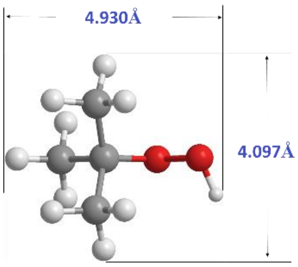
4	**thioanisole**	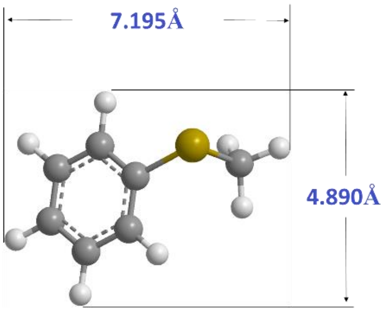

Table S3. QCM data of TBHP/thioanisole adsorption for CBBA-Co coated QCM crystal

Thin film	Sensing film mass (ng)	Adsorbed substance	Mass of adsorbed substance (ng)	Calculated wt%	Theoretical wt%
As prepared CBBA-Co	4270	TBHP	688 (stage 1)	16.1%	14.9%
		thioanisole	123 (stage 2)	2.9%	3.5%

QCM data calculations

According to the Sauerbrey equation, the mass change (Δm) on the surface of quartz crystal is related to the shift in resonance frequency (Δf):

$$\Delta f = -\frac{2nf_0^2}{\sqrt{\rho_q \mu_q}} \times \Delta m = -C_f \times \Delta m$$

where

n = number of the harmonic at which the crystal is driven,

f_o = the resonant frequency of the fundamental mode of the crystal in Hz,

ρ_q = density of quartz = 2.648 g cm^{-3},

μ_q = shear modulus of quartz = 2.947×10^{11} $gcm^{-1} \cdot s^{-2}$.

C_f is called the sensitivity factor for the crystal, and in this study the value of C_f is 56.6 $Hz \cdot \mu g^{-1} cm^2$.

Based on the single X-ray and TG analysis, the formula of CBBA-Co was determined to be $(CBBA)_2 \cdot (Co_3O) \cdot (H_2O)_4 \cdot (DMF)_2$ (M=965.54), the H_2O and DMF molecules were removed upon activation, thus the formula of dehydrated CBBA-Co should be considered as $(CBBA)_2 \cdot (Co_3O)$ (M=965.54 - 4*18.02 - 2*73.09 = 747.3).

In the H_2O adsorption test, the first mass increase stage should be ascribed to the adsorption of coordinated H_2O, ideally four H_2O per CBBA-Co molecule, and the theoretical wt% should be calculated as:

$$\text{wt\%} = \frac{4 \times H_2O}{(CBBA)_2 \cdot (Co_3O)} \times 100\% = \frac{4 \times 18.02}{747.3} \times 100\% = 9.6\% \qquad (1)$$

The slight different of wt% (tested wt%=9.1%) may be caused by the inevitable fast atmosphere moisture uptake. The CBBA-Co thin film was fabricated by spinning coating technology. To thoroughly remove the dispersed isopropanol and all guest molecules of CBBA-Co, the fabricated quartz crystals were firstly treated in high vacuum (<0.01 Pa) at 50 ^{o}C for 3 h prior to test. However, the thin film was inevitably exposed to the air for about a few seconds before being installed into the flow cell adapter, and during this short exposure the sample may take few amount of H_2O from the air, resulting a smaller tested wt% value.

The second mass increase stage should be ascribed to the adsorption of guest H_2O molecules, replacing the original guest DMF. The molecular size of DMF is about 2.5 times of that of H_2O (Table S2), suggesting that theoretically each CBBA-Co molecule should take five guest H_2O molecules. According to this, the theoretical mass increase of this stage should be:

$$\mathrm{wt\%} = \frac{5\times H_2O}{(CBBA)_2\cdot(Co_3O)} \times 100\% = \frac{5\times 18.02}{747.3} \times 100\% = 12.1\% \qquad (2)$$

The tested wt% value is 12.8%, and the slight difference of wt% may be caused by the surface adsorbed H_2O.

In the TBHP (M=90.12) adsorption test, assuming that 50% of the four coordinated H_2O molecules were replaced by the TBHP molecules for each CBBA-Co molecule, thus the theoretical wt% should be

$$\mathrm{wt\%} = \frac{2\times(TBHP-H_2O)}{(CBBA)_2\cdot(Co_3O)\cdot(H_2O)_4\cdot(DMF)_2} \times 100\% = \frac{2\times(90.12-18.02)}{965.54} \times 100\% = 14.9\% \qquad (3)$$

The tested wt% was 16.1%, suggesting that 53% of the H_2O was replaced by TBHP, which is very much close to the assumed value of 50%. In the succeeding thioanisole (M=124.2) adsorption test, considering the limited pore size and the sample had already fully adsorbed with TBHP, the most possible adsorption behavior of thioanisole should be replacing the position of TBHP. The Gaussian calculations also suggest that Co(II) has high affinity towards the S atom. For each CBBA-Co molecule, the above test suggests that 50% of its H_2O was replaced by TBHP. Taking the molecular size into consideration, for every CBBA-Co molecule, it is impossible that all the adsorbed TBHP could be replaced by thioanisole, maximumly only one TBHP of each CBBA-Co molecule could be replaced, thus the theoretical wt% should be 3.5%, which is very close to that of tested value (2.9%).

$$\mathrm{wt\%} = \frac{thioanisole-TBHP}{(CBBA)_2\cdot(Co_3O)\cdot(H_2O)_4\cdot(DMF)_2} \times 100\% = \frac{124.2-90.12}{965.54} \times 100\% = 3.5\% \qquad (4)$$

Table S4. Catalytic activity comparison of CBBA-Co with reported examples in RORs.

	BET Surface area ($m^2 \cdot g^{-1}$)	active site	Temperature (°C)	Catalyst loading	Yield	Time (h)	Stability
REF 33	1600	open Fe/Hf bifunctional sites	55	3%	53% (tandem reaction)	18 (tandem)	/
REF 34	76	open salen Co(III)	r.t.	25 mg for each run, 0.246%	97%	1.5	5 runs
REF 35	/	Fe	80	5%	87%	24	3 runs
This work		potential Co_3O, blocked by coordinated H_2O	70	1%	96%	12	8 runs

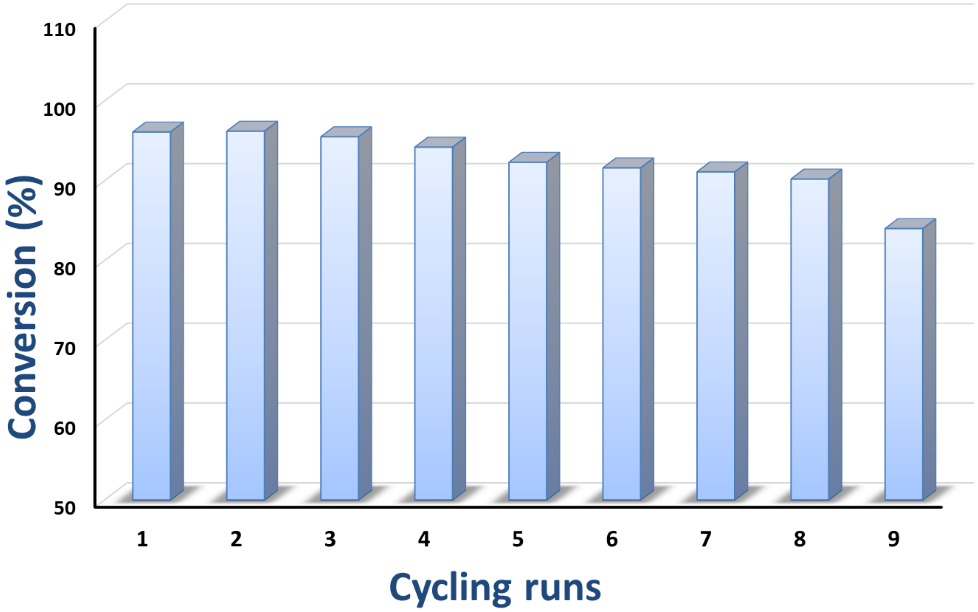

Figure S9. Reusability tests of CBBA-Co on ring opening reaction of cyclohexane oxide with aniline.

Table S5. Catalytic activity comparison of CBBA-Co with reported examples in sulfide oxidation.

	BET Surface area ($m^2 \cdot g^{-1}$)	active site	Temperature (°C)	Catalyst loading	Conversion	selectivity of sulfoxide	Time	stability
REF 35	800	Ta	R.T.	1.20%	85%	90%	>40 h	2 runs
REF 36	850	PW_{12}	45	1.10%	98%	57	20 min	3 runs
REF 37	/	Mo	20	3%	complete conversion	98.60%	3h	/
This work		potential Co_3O, blocked by coordinated H_2O	50	1%	98.80%	>99.9%	12 h	7 runs

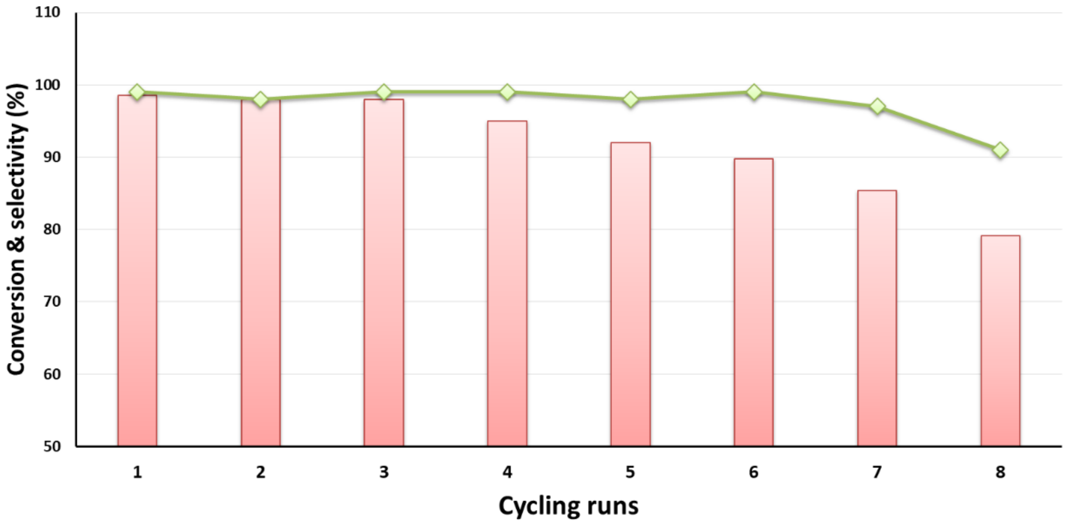

Figure S10. Reusability tests of CBBA-Co on thioanisole oxidation. Red bar: conversion of thioanisole; Green line: selectivity of sulfoxide.

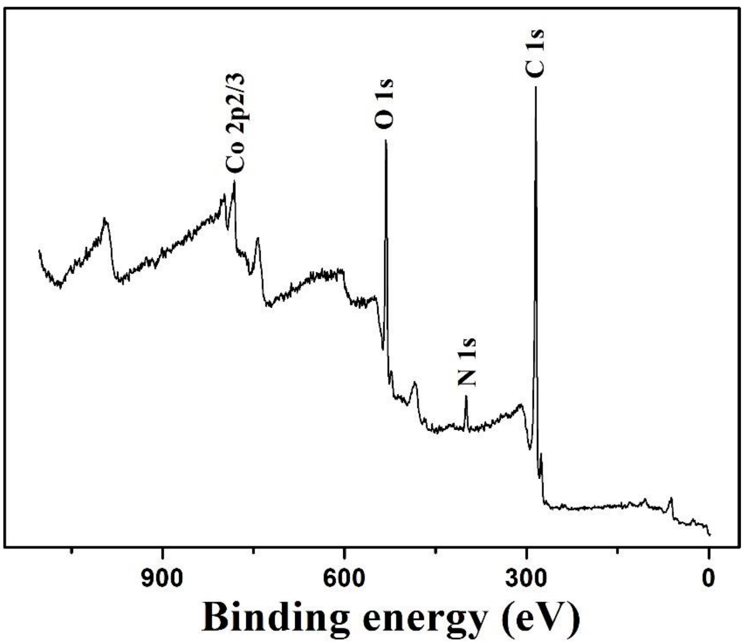

Figure S11. XPS spectra of CBBA-Co after H_2O_2 sensing.